

Direct measurement of molecular stiffness and damping in confined water layers

Steve Jeffery,^{1,*} Peter M. Hoffmann,^{2,†} John B. Pethica,^{1,‡} Chandra Ramanujan,¹ H. Özgür Özer,³ and Ahmet Oral⁴

¹*Department of Materials, University of Oxford, Parks Road, Oxford OX1 3PH, United Kingdom*

²*Department of Physics, Wayne State University, 666 W. Hancock, Detroit MI 48201, USA*

³*Department of Physics, Trinity College, Dublin, Ireland*

⁴*Department of Physics, Bilkent University, Ankara, Turkey*

(Dated: November 14, 2018)

We present *direct* and *linear* measurements of the normal stiffness and damping of a confined, few molecule thick water layer. The measurements were obtained by use of a small amplitude (0.36 Å), off-resonance Atomic Force Microscopy (AFM) technique. We measured stiffness and damping oscillations revealing up to 7 layers separated by 2.56 ± 0.20 Å. Relaxation times could also be calculated and were found to indicate a significant slow-down of the dynamics of the system as the confining separation was reduced. We found that the dynamics of the system is determined not only by the interfacial pressure, but more significantly by solvation effects which depend on the exact separation of tip and surface. Thus ‘solidification’ seems to not be merely a result of pressure and confinement, but depends strongly on how commensurate the confining cavity is with the molecule size. We were able to model the results by starting from the simple assumption that the relaxation time depends linearly on the film stiffness.

PACS numbers: 68.08.-p, 07.79.Lh, 62.10.+s, 61.30.Hn

I. INTRODUCTION

The structure of water, as the primary biological solvent, has been intensively studied. For example, liquid water adopts short-range order, which depends strongly on dissolved species or geometric constraints. This structure emerges from the minimization of the free energy associated with the dynamic system of hydrogen bonds between neighboring water molecules. The entropy cost of the induced order almost certainly plays an important role in determining the structure of biological molecules that depend on hydration for their function, such as proteins and cell membranes¹.

A surface can act as a model system for studying these phenomena, as it is both geometrically disrupting and can be chemically functionalized to affect the structure of the water close to it. A particularly interesting problem is the emergence of density oscillations as a function of film thickness when water is confined between two surfaces². This phenomenon is related to the radial density fluctuations in solvation shells of solutes. These density fluctuations have been originally observed by diffraction methods in clay-water systems^{3,4}.

In 1982, the mechanical response of confined water layers was directly determined using the Surface Force Apparatus (SFA)⁵. With the invention of the Atomic Force Microscopy (AFM), attempts were made to measure stiffness oscillations with this technique⁶. AFM probes have a much smaller contact area than SFA. This is an advantage if local changes in the water structure are to be examined⁷, and potentially allows for probing regions of negative contact stiffness. The latter cannot be probed using SFA, because the instrument stiffness is not high enough to withstand the snap-in instability in negative stiffness regions. The disadvantage of AFM is that the signals are much smaller and the contact area is deter-

mined by the tip shape and thus is essentially unknown. The small signal-to-noise ratio in AFM made the direct measurement of water structure an elusive goal. In 1995, Cleveland et al.⁸ measured the oscillatory potential of the confined water layers indirectly by analyzing the Brownian noise spectrum of a AFM tip immersed in water. More recently, direct measurements of the structure were achieved by Jarvis et al.⁹ by using nanotube probes and a large amplitude AFM technique, and by Antognozzi et al.¹⁰ who measured the local shear modulus using an AFM in shear force mode.

In this paper we present results of direct and *linear* measurements of the normal junction stiffness of water confined between the AFM tip and an atomically smooth mica surface. This was achieved by using ultra-small amplitudes of 0.36 Å and sub-resonance operation, which avoids the problem of reduced quality factor in liquids. The snap-in instability was avoided by using a sufficiently stiff cantilever (here 0.65 N/m). This method is ideal to make quantitative, point-by-point measurements of the mechanical properties of confined water layers. The small amplitudes (much smaller than the nominal size of a water molecule) allow us to measure the elastic and viscous response of the confined water layer without disrupting the layers themselves, as would be the case in the large amplitude methods used previously. The challenge of such a technique is the measurement of exceedingly small signals, since the usual methods of signal enhancement (large amplitudes, low stiffness levers, resonance operation) are not used. Recently, we succeeded in implementing such a technique in UHV^{11,12,13} - and in liquids¹⁴, using an improved fiber interferometric displacement sensor¹⁵ to overcome the reduced signal-to-noise of the technique. Here we report on our direct measurements of the mechanical properties of confined water layers using this novel AFM technique.

II. EXPERIMENTAL

Small amplitude, off-resonance AFM¹¹ has recently been successfully used for measuring atomic bonding curves¹², mapping force gradients at atomic resolution¹³, and measuring atomic scale energy dissipation¹⁶. Both the force gradient and the damping coefficient/ energy dissipation can be obtained by solving the equation of motion for a forced damped oscillator at a drive amplitude $A_0 \ll \lambda$ (where λ is the nominal range of the measured interaction) and $\omega \ll \omega_0$. The equation of motion is given by:

$$m\ddot{x} + \gamma\dot{x} + (k_L + k)x = k_L A_0 \exp(i\omega t) \quad (1)$$

where we linearized the force field, owing to the fact that lever amplitudes are much smaller than the range of the measured interactions, λ . This assumption has recently been shown to be justified if A_0 is sufficiently small¹⁷. After solving the equation, we find for the interaction stiffness and the damping coefficient:

$$k = k_L \left(\frac{A_0}{A} \cos \phi - 1 \right) \quad (2)$$

and

$$\gamma = -\frac{k_L A_0}{A\omega} \sin \phi \quad (3)$$

Here, A_0 is the drive amplitude of the lever, A is the measured amplitude as the surface is approached, k_L is the lever stiffness, ϕ is the measured cantilever phase, and k is the measured interaction stiffness. In equation (3), ω is the drive frequency and γ is the damping coefficient. In performing the above calculations, we intrinsically assume that elastic and viscous forces are additive, i. e. they act in parallel (Kelvin model). In modeling liquids, however, typically a Maxwell model is used in which the elastic and viscous (damping) term are considered to be in series. To convert from one to the other we can use the following set of equations¹⁸:

$$\eta = \gamma + \frac{k^2}{\omega^2 \gamma} \quad (4)$$

$$R = k + \frac{\omega^2 \gamma^2}{k} \quad (5)$$

where η and R are the viscous and elastic terms in the Maxwell model, respectively.

The used AFM was home-built and incorporated a fiber interferometer mounted on a remote controlled nano-manipulator with 5 degrees of freedom and a step size of < 100 nm. The nominal sensitivity of the interferometer was $3 \times 10^{-4} \text{ \AA} / \sqrt{\text{Hz}}$. This allowed us to measure stiffnesses of a few 10^{-2} N/m using a 0.65 N/m cantilever, a sub-Angstrom lever amplitude of 0.36 Å and reasonable integration times. The measurement frequency was 411 Hz. Measurements were performed in ultrapure water with a concentration of 0.01 M KCl. The surface was freshly cleaved mica, and the cantilever tip was made out of silicon.

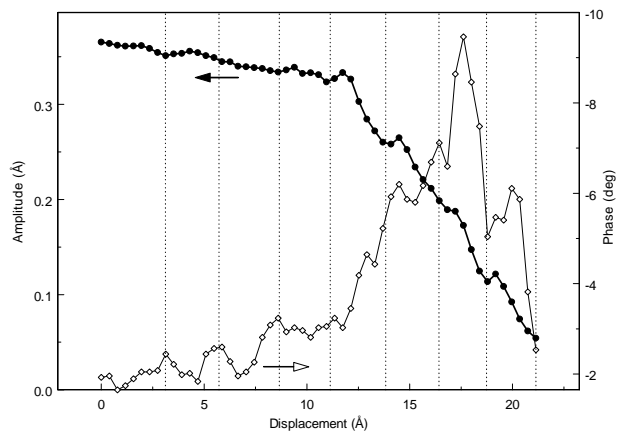


FIG. 1: Amplitude and phase measured on a water layer confined between the AFM tip and a mica surface. The mica surface is located to the right. Several oscillations can be seen in the amplitude data. The overall decrease as the surface is approached is due to hydrophilic effects. The phase shows a more complicated behavior (discussed in text), but also shows clear oscillations. The reference lines correspond to displacements where liquid ordering is maximized and serve as a guide for the eye.

III. RESULTS

Figure 1 shows the amplitude and the cantilever phase as a function of displacement. The surface is located to the right of the graph, and the monotonic drop-off of the amplitude as the surface is approached can be attributed to repulsive interactions, which are most likely hydrophilic in origin. The amplitude data shows at least 5 equally spaced local minima (and maxima). The phase data shows equally spaced maxima further away from the surface, which roughly line up with the minima of the amplitude data. However, as the surface is further approached additional ‘intermediate’ peaks appear close to the amplitude maxima, and these peaks finally dominate as the gap is decreased to a few molecular spacings. The average spacing between the amplitude minima (and the phase maxima further out) is $2.56 \text{ \AA} \pm 0.20 \text{ \AA}$, consistent with earlier reports^{5,7,8,9,10}. Overall, the phase increases up to a global maximum as the surface is approached and then decreases again closer to the surface.

The measured stiffness (equation (2)) can be decomposed into two components: A monotonic background, and an oscillatory term, which is the one we will be most concerned with in this paper. The monotonic background is most likely due to double-layer (DVLO) and hydrophilic interactions, which can both be modelled as exponentials. A best fit and subsequent subtraction of the monotonic background yields the data shown in Figure 2. Also shown in Figure 2 is the damping coefficient calculated using equation (3). Note that the peaks in the stiffness data correspond to the minima in the amplitude data and thus to the higher stiffness of the ordered

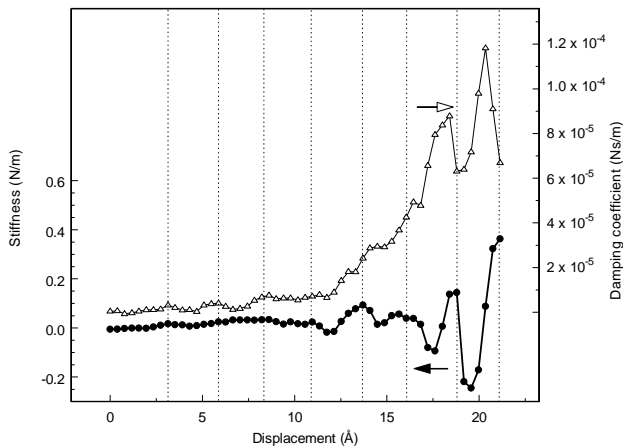


FIG. 2: Solvation stiffness and (Kelvin) damping coefficient versus displacement. The solvation stiffness was obtained by calculating the stiffness from equation (2) and subtracting the exponential background. Again, clear oscillations spaced at 2.56 \AA can be seen in both the stiffness and the damping. The damping exhibits a ‘phase-shift’ with respect to the stiffness data at a displacement of 15 \AA . Closer to the surface the damping is out-of-phase with the stiffness, while further away it switches to being in-phase.

phase of the confined water layer. Close to the surface, the damping curve shows peaks that are ‘out of phase’ with the stiffness data. Further away from the surface, however, double peaks occur, and finally the damping shows peaks that are in-phase with the stiffness maxima, similar to the phase data shown in Figure 1. Due to the dissipation, the cantilever loses kinetic energy. The energy loss per cycle can be calculated from¹⁹

$$E_{\text{diss}} = \oint_{\text{cycle}} \gamma \dot{x} = \pi \gamma \omega A^2 = \pi k_L A_0 A \sin \phi \quad (6)$$

The maximum loss was $E_{\text{diss}} = 1.3 \text{ meV}$ per cycle, which was observed close to the maximum in the phase (Figure 1).

What is the origin of the observed dissipation and its increase as the surface is approached? One interpretation would be to attribute the damping to viscous drag, especially due to the squeezing of the liquid between the tip and the substrate²⁰. The squeeze Reynolds number, Re , is given by:

$$Re = \frac{\rho_W z}{\eta_W} \frac{dz}{dt} \quad (7)$$

where η_W is the viscosity of water, ρ_W is its density, and z is the tip-surface distance. In our case, $z \approx 1 \text{ nm}$, $dz/dt \approx \omega A \approx 100 \text{ nm/s}$ and we obtain $Re \approx 10^{-10} \ll 1$. In the following we assume that the viscous damping due to the cantilever beam does not change much with separation (since the beam is several micrometers away), and thus the variation of the damping with separation is dominated by the damping at the tip. With $Re \ll 1$, the

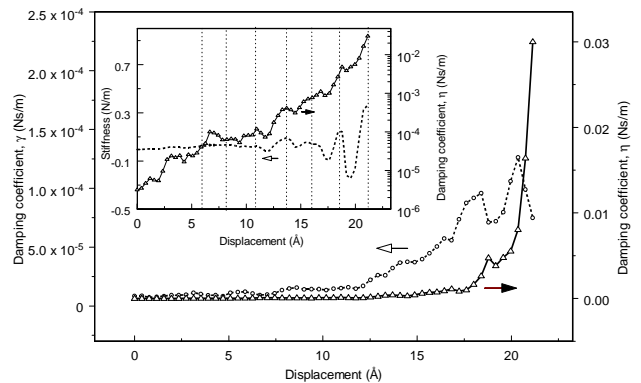


FIG. 3: Comparison of Kelvin damping, γ , and Maxwell damping, η . If we treat the confined film as a liquid (Maxwell-type model), we find that the damping increases very strongly as the film is squeezed to a few molecular layers, unlike the Kelvin damping which increases more moderately. The inset shows the Maxwell damping, η , on a log- scale, with the stiffness as a reference. It can be seen that η is essentially in-phase with the stiffness throughout the measurement range.

squeeze damping term between tip and surface is given by²⁰:

$$\gamma_s = 6\pi\eta_W \frac{R_{\text{tip}}^2}{z} \quad (8)$$

Using reasonable values (10-100 nm) for the tip radius, R_{tip} , we find that the expected viscous damping at less than 1 nm separation is of the order of 10^{-9} to 10^{-7} Ns/m, which is about three to four orders of magnitude smaller than the measured values (see Figure 2), which are of order 10^{-5} to 10^{-4} Ns/m. We found that the viscosity increased exponentially with distance and thus is large only very close to the surface ($< 1 \text{ nm}$). This effect has been observed before and has been attributed to a sharp increase in the effective viscosity of confined liquid layers^{10,20,21}, a possible indication of the altered dynamical and structural properties of liquids under confinement. However, Raviv et al.^{22,23} recently observed viscosities close to the bulk value even at separations as small as 1 nm. Their results were based on measurements of the snap-in instability close to the surface, while in the present experiment the mechanical properties of the film were measured continuously without any mechanical instabilities. Moreover, in our experiment we considered normal forces, while their results are based on shear measurements. How these measurements relate to each other and if there is a fundamental difference between the normal and the lateral dynamic behavior of water is an important question for future study.

Another debate has been the nature of the structural and dynamical differences between confined and bulk liquids. The difference has been attributed to a type of first-order phase transformation from liquid to solid²⁴, or, alternatively, to a continuous transformation, not unlike a glass transition²⁵. If the liquid does indeed turn solid un-

der certain confinement conditions, the proper mechanical model would be a Kelvin-type model. However, if the liquid stays essentially liquid albeit with greatly enhanced viscosity (recent evidence for this comes from diffusion measurements²⁶), a Maxwell-type model should be used. As in any ‘standard’ analysis of AFM, we used a Kelvin-type model above. However, to elucidate the nature of the changes under confinement further, it is important to use a model that properly applies to liquids. Using equations (4) and (5) we transformed the measured stiffness and damping terms to the Maxwell model. We found that the stiffness remains almost unchanged between the two models (i. e. $k \approx R$), but as shown in Figure 3, the viscous term changes dramatically. The Kelvin model damping term, γ , is out-of-phase with the stiffness oscillations close to the surface (Figure 2), while the Maxwell model damping, η , is much larger and essentially in-phase with the stiffness variations (Figure 3). As mentioned above, further away from the surface, the Kelvin damping experiences a ‘phase shift’ and becomes in-phase with the stiffness (similar to the phase data in Figure 1). The Maxwell damping, on the other hand, remains in-phase through-out. More about this below.

When dealing with dissipative behavior it is useful to look at the characteristic time constants involved in the dynamic behavior of the confined liquid. In the Kelvin model, a characteristic time is given by $t_c = \gamma/k$, which is called the ‘retardation time’¹⁸. This time is approximately the time needed to build up a significant strain in the material upon application of a constant stress. In standard solids, a certain amount of strain can be obtained almost instantaneously due to the elasticity of the material, however, in ideal liquids, instantaneous strain is not possible due to the velocity-dependent damping. Thus a lower t_c might indicate a more solid-like material. On the other hand, in the Maxwell model, the characteristic time is $t_r = \eta/R$, which is the ‘relaxation time’. This time is related to the time needed for stresses in the material to relax after a strain has been imposed. In solids, stresses will persist for long times when a strain is applied (one of the characteristic of materials being solid), while in liquids any stresses will quickly dissipate away. Thus higher t_r indicates a more solid-like behavior. It should be noted that t_c and t_r are simply related by:

$$t_c = \frac{1}{\omega^2} t_r \quad (9)$$

The dependence of t_c and t_r on displacement is shown in Figure 4. It can be seen that overall t_c is decreasing and t_r increasing as the liquid layer is increasingly confined. This indicates a tendency for the layer to become more solid-like. Even more interesting, however, is the fact that at separations where the stiffness oscillations are at their maximum, t_c is lowered and t_r is increased. This is a further indication that the water becomes more solid-like when it is allowed to order, i. e. when the tip-surface separation is commensurate with the ‘natural’ molecular

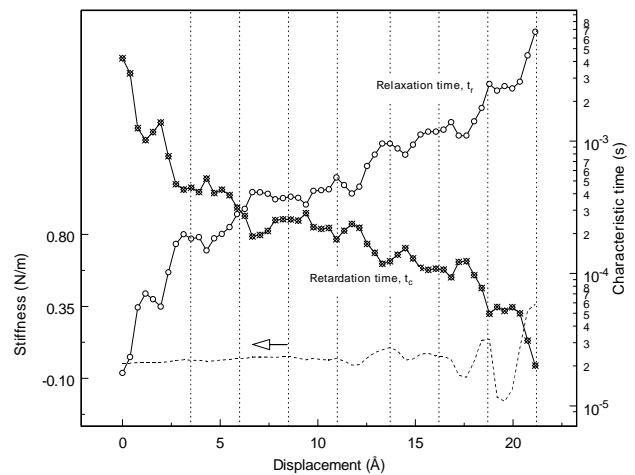


FIG. 4: Relaxation (t_r) and retardation (t_c) time plotted versus displacement. The relaxation time is in-phase with the stiffness, while the retardation time is out-of-phase. The relaxation time increases overall due to the increasing pressure, but also exhibits in-phase oscillations due to solvation effects.

spacing of water. In the ‘ordered phase’, the stiffness k (or R) is maximum, the retardation time, t_c , is minimum, and the relaxation time, t_r , is maximum, as expected for a solid.

Another interesting observation is that the characteristic times t_r and t_c change very slowly with separation until a few Angstrom from the surface. Then they seem to change more rapidly, with the liquid becoming seemingly even more solid-like. Some authors²⁴ have argued that this behavior shows the liquid undergoes some kind of first order phase transformation upon confinement, while others suggest a more gradual, glass-like transition²⁵. Recent results measured under shear even suggest that water in particular fails to ‘solidify’ at all²¹. Based on our results we cannot conclusively decide between these viewpoints. However, as we will see below, there seems to be both a gradual stiffening of the layer as pressure is applied and a much more pronounced periodic change of the mechanical behavior of the layer.

IV. DISCUSSION AND MODEL

There are several surprising findings from the linear measurement of confined water presented here: 1) Observed oscillations in the phase and dissipation extend much further than the oscillations in the amplitude or stiffness, 2) the phase and the Kelvin damping oscillations experience a ‘phase shift’ with respect to the stiffness data as we move away from the surface, 3) while on average the amplitude continuously decreases as the surface is approached, the phase seems to pass through an intermediate maximum, and, finally, as hinted above, 4)

the mechanical behavior of the layer changes both gradually (hydrophilic background) and more abruptly (solvation shell oscillations). To explain this behavior we simulated the nanomechanical behavior of the water layer by starting from the assumption that the relaxation time, t_r , is to first order linearly dependent on the stiffness of the water layer. This is not to be taken literally, in the sense of a direct physical connection between the stiffness and the relaxation time (although there well might be), but rather the stiffness is seen as an indicator of the ‘solidness’ of the layer, and the relaxation time (as another indicator) is taken to be essentially proportional to it. We found that we can get the best fit of our data if we assume that the relaxation time depends linearly on both the background stiffness, k_h , due to hydrophilic interaction and on the stiffness oscillations, k_s , due to the solvation effects but with two different ‘coupling’ constants α_1 and α_2 :

$$t_r = \alpha_1 k_h + \alpha_2 k_s + t_0 \quad (10)$$

Here, t_0 corresponds to the relaxation time measured far away from the surface. The advantage of using separate constants α_1 and α_2 is that we can separate the effect of background hydrophilic interactions from the influence of solvation forces on the relaxation time. We found that in order to reproduce the experimental results as closely as possible it was necessary to set α_1 to 2.3×10^{-3} sm/N and α_2 to 5×10^{-3} sm/N, i. e. the relaxation time was more than twice as sensitive to solvation forces than it was to the hydrophilic background. It should be noted that the hydrophilic background stiffness is directly proportional to the load (or surface pressure), since both are exponentials and one is the derivative of the other. Thus by the above approach we can separate the effects of the overall pressure or load from the effect of the liquid ordering which only occurs at certain, molecularly commensurate separations.

The retardation time, t_c , can be calculated from equation (9). The damping coefficients γ and η are then given by:

$$\gamma = t_c \cdot k \quad (11)$$

$$\eta = t_r \cdot R \quad (12)$$

In the simulations, we took $k = R$ (as found experimentally) to simplify the calculations. The solvation force was modeled as follows²:

$$F_s = \sum_{\text{tip}, k=0}^N 2\pi r^2(z_k) \cdot k_B T \rho \cos\left(\frac{2\pi(z_k + D)}{\sigma}\right) \exp\left(-\frac{z_k + D}{\sigma}\right) \quad (13)$$

where we summed the contributions of different areas of the tip by subdividing the tip into N horizontal ‘slices’ of radius $r(z_k)$. Here, ρ is the particle density of water, σ is both the period and the decay parameter of the interaction (they were experimentally found to be nearly

identical), z_k is the height of the k ’th slice of the tip, and D is the tip-surface separation. The hydrophilic interaction is given by:

$$F_h = \sum_{\text{tip}, k=0}^N 2\pi r^2(z_k) \cdot p_h \exp\left(-\frac{z_k + D}{\lambda}\right) \quad (14)$$

where p_h is a constant and λ is the decay parameter of the hydrophilic background. All parameters in expressions (13) and (14) were determined from the experiment. The hydrophilic decay parameter was found to be only slightly smaller ($\lambda = 2.45\text{\AA}$) than the decay parameter of the oscillations ($\sigma = 2.56\text{\AA}$). The corresponding stiffnesses were found from taking the derivative of the forces with respect to tip-surface separation, $k = -dF/dD$.

Since we cannot know the exact geometry of the tip, we did not expect to get a perfect agreement between theory and experiment. Nevertheless we obtained a semi-quantitative agreement that reproduces all of the surprising features mentioned above. The geometry of the tip was assumed to be paraboloid, and the best agreement with experimental data was obtained for a nominal radius of 1nm. Figure 5 shows the calculated total stiffness and Kelvin damping coefficient, γ . The damping coefficient is out-of-phase with the stiffness close to the surface, then undergoes a ‘phase shift’ and becomes in-phase close to the surface, as seen in the experiment. From equation (11) we see that the damping is a product of the retardation time, t_c and the stiffness, k . Close to the surface the damping is dominated by the retardation time t_c , which is always out-of-phase with the stiffness (Figure 4), while further away from the surface the stiffness k dominates the variation in the damping. On the other hand, the Maxwell damping, η , is always in phase with the stiffness, since the relaxation time t_r is in-phase with R (or k).

It can be shown that a more complicated mechanical model, such as the commonly used Burger’s model, behaves like a Maxwell model at low frequencies. This implies that the present discussion has more general implications than might be expected from the use of such simplified mechanical models. In particular, it would seem from equation (11) that the oscillatory behavior of the Kelvin damping, γ , could be explained by the oscillatory behavior of the stiffness, even if the retardation time is constant or slowly varying. In this scenario, the observed oscillations of the retardation/relaxation time would be merely an ‘artifact’ of the calculation. However, if the retardation time were constant or smoothly varying (i.e. not oscillating), the Kelvin damping would have to remain in-phase with the stiffness at all times. This is not observed in the experiment. The fact that γ is out-of-phase close to the surface implies that the relaxation/retardation time of the liquid exhibits separation-dependent oscillations independent of the oscillations of the stiffness. This means that the *dynamic* behavior of the confined liquid is strongly affected by how commensurate the tip-surface spacing is with regard to the size

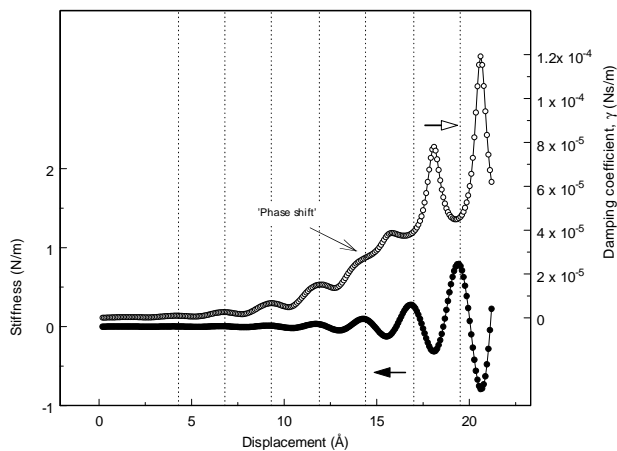


FIG. 5: Simulated stiffness and Kelvin damping, γ . Compare to measured data (Figure 2). Although we had to assume larger stiffness oscillations in the model, the overall agreement is good, and the ‘phase shift’ in the damping data is reproduced well.

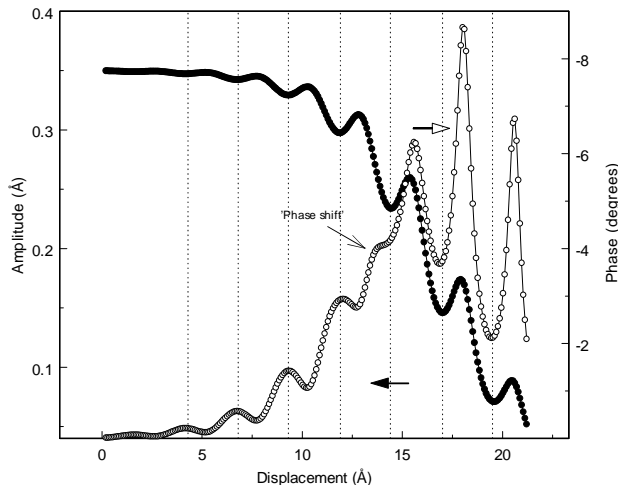


FIG. 6: Simulated amplitude and phase. Compare to measured data (Figure 1). There is good qualitative agreement and the complicated behavior of the phase is well reproduced including the ‘phase shift’ with respect to the stiffness (here: amplitude) and the global maximum.

of the confined molecules.

The phase was calculated by solving equations (2) and (3) simultaneously (and assuming $\omega \ll \omega_0$):

$$\tan \phi = \frac{\omega \gamma}{k + k_L} \quad (15)$$

The simulated phase, ϕ , is shown in Figure 6. The simulation reproduces all the ‘puzzling’ features of the experiment: The shift from being out-of-phase to being in-phase with the stiffness oscillations and the intermediate maximum in the phase. The shift is due to the shift in γ discussed above. The intermediate maximum is due to the fact that the stiffness changes slowly far from the surface, but then rather rapidly closer in, ‘overtaking’ the damping coefficient in the process (equation (15)). The observation that oscillations in the phase or damping are observable further away from the surface than the oscillations of the stiffness can also be explained: As we can see in the simulated phase, a phase of more than 1° is observed as far away as 13\AA from the closest approach (about 5 water layers). Such a phase angle can be easily measured with a lock-in amplifier. On the other hand, at the same separation, the stiffness is only 0.04 N/m requiring a measurement of a change in lever amplitude of the order of 0.02\AA , which is more difficult to measure and can be lost in the noise.

In conclusion, we can see that our simple approach of directly relating the relaxation time to the stiffness of the layer has allowed us to reproduce all the important features of the experiment. The relaxation/retardation times can therefore be taken as fundamental physical parameters (together with the stiffness) that characterize the mechanical properties of the system quite well. The weaker dependence of the relaxation time on the hydrophilic interaction and the more pronounced dependence on solvation forces, suggests a compromise in the continuing debate over the nature of the solid-liquid transition. It seems that there is a gradual increase of the relaxation time with surface pressure and a more substantial change related to the molecular ordering of the liquid close to the surface.

* Current address: Oak Hill Theological College, Southgate, London N14 4PS, UK

† Electronic address: hoffmann@physics.wayne.edu

‡ Current address: Department of Physics, Trinity College, Dublin, Ireland

¹ J. L. Finney, *Faraday Discuss. Chem. Soc.* **103**, 1 (1996).

² J. N. Israelachvili, *Intermolecular & Surface Forces* (Academic Press, London, 1992), chapter 13.

³ W. F. Bradley, R. E. Grim, and G. L. Clark, *Z. Krist.* **97**, 216 (1937).

⁴ U. Del Pennino, E. Mazzega, S. Valeri, A. Aliette, M. F. Brigatti, and L. Poppe, *J. Colloid Interface Sci.* **84**, 301

(1981).

⁵ J. N. Israelachvili and R. M. Pashley, *Nature* **306**, 249 (1983).

⁶ S. J. O’Shea, M. E. Welland, and T. Rayment, *Appl. Phys. Lett.* **60**, 2356 (1992).

⁷ D. L. Patrick and R. M. Lynden-Bell, *Surf. Sci.* **380**, 224 (1997).

⁸ J. P. Cleveland, T. E. Schäffer, and P. K. Hansma, *Phys. Rev. B* **52**, R8692 (1995).

⁹ S. P. Jarvis, T. Uchihashi, T. Ishida, H. Tokumoto, and Y. Nakayama, *J. Phys. Chem. B* **104**, 6091 (2000).

¹⁰ M. Antognozzi, A. D. L. Humphris, and M. J. Miles, *Appl.*

- Phys. Lett. **78**, 300 (2001).
- ¹¹ A. Oral, R. A. Grimble, H. Ö. Özer, and J. B. Pethica, Rev. Sci. Instr. **74**, 3656 (2003).
- ¹² P. M. Hoffmann, A. Oral, R. A. Grimble, H. Ö. Özer, S. Jeffery, and J. B. Pethica, Proc. R. Soc. Lond. A **457**, 1161 (2001).
- ¹³ A. Oral, R. A. Grimble, H. Ö. Özer, P. M. Hoffmann, and J. B. Pethica, Appl. Phys. Lett. **79**, 1915 (2001).
- ¹⁴ P. M. Hoffmann, S. Jeffery, A. Oral, R. A. Grimble, H. Ö. Özer, and J. B. Pethica, Mat. Res. Soc. Symp. Proc. **649**, Q9.2 (2001).
- ¹⁵ D. Rugar, H. J. Mamin, and P. Guethner, Appl. Phys. Lett. **55**, 2588 (1989).
- ¹⁶ P. M. Hoffmann, S. Jeffery, J. B. Pethica, H. Ö. Özer, and A. Oral, Phys. Rev. Lett. **87**, 265502 (2001).
- ¹⁷ P. M. Hoffmann, Appl. Surf. Sci. **210**, 140 (2003).
- ¹⁸ W. N. Findley, J. S. Lai, and K. Onaran, *Creep and Relaxation of Nonlinear Viscoelastic Materials* (Dover, New York, 1976), chapter 5.
- ¹⁹ B. Anczykowski, B. Gotsmann, H. Fuchs, J. Cleveland, and V. B. Elings, Appl. Surf. Sci. **140**, 376 (1999).
- ²⁰ S. J. O'Shea and M. E. Welland, Langmuir **14**, 4168 (1998).
- ²¹ Y. Zhu and S. Granick, Phys. Rev. Lett. **87**, 096104 (2001).
- ²² U. Raviv, P. Laurat, and J. Klein, Nature **413**, 51 (2001).
- ²³ U. Raviv and J. Klein, Science **297**, 1540 (2002).
- ²⁴ J. Klein and E. Kumacheva, J. Chem. Phys. **108**, 6996 (1998).
- ²⁵ A. L. Demirel and S. Granick, Phys. Rev. Lett. **77**, 2261 (1996).
- ²⁶ A. Mukhopadhyay, J. Zhao, S. C. Bae, and S. Granick, Phys. Rev. Lett. **89**, 136103 (2002).